Dynamical and quasistatic structural relaxation paths in $Pd_{40}Ni_{40}P_{20}$ glass

A. Kahl,[1,2] T. Koeppe,[1] D. Bedorf,[1] R. Richert,[3] M. L. Lind,[2] M. D. Demetriou,[2] W. L. Johnson,[2] W. Arnold,[1] and K. Samwer[1,a)]
[1]*I. Physikalisches Institut, Universität Göttingen, D-37077 Göttingen, Germany*
[2]*Keck Laboratory, MS 187-36, Caltech, Pasadena, California 91125, USA*
[3]*Department of Chemistry and Biochemistry, Arizona State University, Tempe, Arizona 85287, USA*

(Received 28 August 2009; accepted 29 October 2009; published online 19 November 2009)

By sequential heat treatment of a $Pd_{40}Ni_{40}P_{20}$ metallic glass at temperatures and durations for which α-relaxation is not possible, dynamic, and quasistatic relaxation paths below the glass transition are identified via *ex situ* ultrasonic measurements following each heat treatment. The dynamic relaxation paths are associated with hopping between nonequilibrium potential energy states of the glass, while the quasistatic relaxation path is associated with reversible β-relaxation events toward quasiequilibrium states. These quasiequilibrium states are identified with secondary potential energy minima that exist within the inherent energy minimum of the glass, thereby supporting the concept of the sub-basin/metabasin organization of the potential-energy landscape. © *2009 American Institute of Physics*. [doi:10.1063/1.3266828]

In recent years, descriptions of the structural kinetic behavior of metallic liquids and glasses have been significantly revisited.[1] It became evident that various secondary structural relaxation modes instead of a single primary one are necessary to accurately describe the entire dynamic behavior of a metallic glass.[2] These secondary structural relaxation modes, termed Johari–Goldstein or slow β-modes, and the primary structural relaxation termed α-mode merge at a temperature above the glass transition specific for each material. This merging temperature is very close to the critical temperature of mode-coupling theory.[3] At lower temperatures, the onset of the glass transition depends on the cooling rate[4] or the external frequency.[5] The viscosity of the material tends to follow a Vogel–Fulcher–Tammann (VFT) law upon cooling,[6] until the α-relaxation mode "freezes" at T_g on experimental time scales of $\approx$100 s. The predicted divergence of the relaxation time at a finite VFT-temperature remains inconsequential, as has recently been demonstrated in a careful analysis of viscosity data.[7] In contrast, the slow β- or Johari–Goldstein mode is believed to be responsible for low-temperature diffusion,[8] which is found to operate at temperatures as low as 200 °C below T_g.[2] In the past, changes in Young's modulus,[9] decrease in free volume,[10] or irreversible effects in the diffusion mechanism in as-quenched samples have been attributed to the β-relaxation mode in these alloys,[3] suggesting that aging is a cooperative phenomenon as described in many earlier molecular dynamics simulations.[11] In a recent paper,[12] these secondary β-relaxation events were identified with reversible anelastic excitations within the elastic matrix confinement, and an α-relaxation event was identified with the collapse of the matrix confinement and the breakdown of elasticity, a view consistent with Eshelby's concept of elastic confinement.[13] In a different approach Khonik *et al.*[14] showed very recently, that structural relaxation can change significantly the concentration of so called interstitiallylike defects leading also to a distinct change of the shear modulus depending on the quenched, annealed or initial condition of the sample. In this paper, we provide evidence that not only the dynamic aging process is clearly identified by ultrasonic measurements, but also the rejuvenation process toward distinct quasiequilibrium sub-basins is detectable when the system is relaxed by thermal β-excitations below the dissipative α-relaxation transition.

The PdNiP glass was prepared by prealloying Pd (99.95%) and Ni (99.95%) by arc melting in argon atmosphere. The arc-melted ingot was then sealed in a quartz tube under argon atmosphere together with P (99.999%) and B_2O_3, which was used as a fluxing agent. After inductively melting the components, the alloy was cast into a 7-mm-diameter rod that was cut and polished to a length of about 6 mm with the upper and lower ends as parallel as possible to obtain high-precision ultrasonic measurements. X-ray diffraction (Siemens D5000) and differential scanning calorimetry (DSC) (Perkin Elmer DSC-7) scans were performed to confirm the amorphicity of the sample. From the DSC scans we determined the onset of the calorimetric glass transition and crystallization for a heating rate of 10 °C/min to be at 296 and 390 °C, respectively. The density of the sample was measured using a *Brand* pycnometer following Archimedes method and found to be 9.32 ± 0.05 g/cm^3, a value slightly lower than previously reported values. The composition of the amorphous alloy was verified by EDX measurements in a Supra 35 (Zeiss) with an EDX system (Thermo Electron). The results at different points of the sample averaged to $Pd_{40.5\pm0.2}Ni_{40.6\pm0.3}P_{18.9\pm0.2}$. To investigate the temperature dependence of the isoconfigurational shear modulus, we carried out a series of hourly annealing processes followed by ultrasonic measurements. After an hourly isothermal annealing process at temperature T_a, the sample was rapidly water quenched to freeze-in the configurational state of the system at T_a. The room-temperature shear velocity of sound was measured *ex situ* on the quenched sample using the ultrasonic pulse-echo overlap method using a shear-wave piezoelectric transducer (see Fig. 1). A 6 MHz PZT AZ Roditi transducer is employed to generate ultrasonic pulses using a Matec Model 6600 pulse modulator and receiver monitored by a gigahertz-bandwidth digital oscilloscope.[8] Each individual maximum in the tone-burst pulse (up to 12) is used to

a)Electronic mail: ksamwer@gwdg.de.

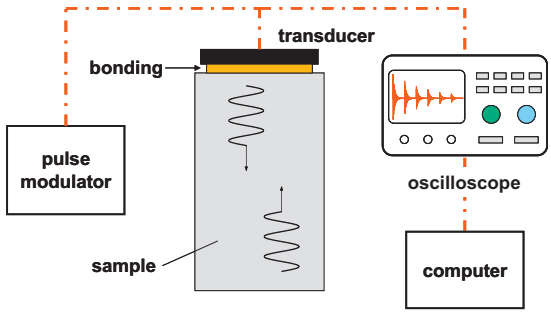

FIG. 1. (Color) Experimental setup for ultrasonic pulse-echo measurements at room temperature.

calculate the time-of-flight of the pulse. In this manner, the error in sound velocity is minimized.

Figure 2 shows the room-temperature shear modulus calculated from the time-of-flight data, the density, and the length of the sample, plotted against the temperature at which the sample has been annealed, T_a. We would like to note here that the overall trends in G discussed below are well outside the average measurement error, which we denote by error bars in Fig. 2. The first cycle of one-hour annealing steps was performed at temperatures between 50 and 290 °C using a single as-quenched sample. Each step was followed by water quenching and ultrasonic measurement at room temperature. The 18 1 h measurements of the first cycle are indicated by filled circles in Fig. 2. Below 280 °C, a small but consistent increase in the shear modulus G from about 36.5 to 37.5 GPa can be observed, while above 280 °C a steep decrease down to 37.0 GPa is evident. This steep decrease is identified with the α-relaxation process, which becomes possible when the sample is annealed at temperatures above 280 °C for one hour durations. The α-relaxation path indicated by data that correspond to hourly annealing processes above 280 °C is denoted by a solid line in Fig. 2. Using the same sample, we then performed a second cycle of one-hour annealing experiments, starting from 150 to 280 °C. In the second cycle, the initial G-value starts higher (37.3 GPa), passes through a maximum near 220 °C, and then begins a downward trend which becomes rather steep just above 275 °C. Finally, a third one-hour annealing cycle is performed using the same sample, and qualitatively the same behavior can be observed: G starts at 37.8 GPa, passes through a maximum at 200 °C, and finally enters a downward trend before the glass transition is reached and a rapid decrease is seen.

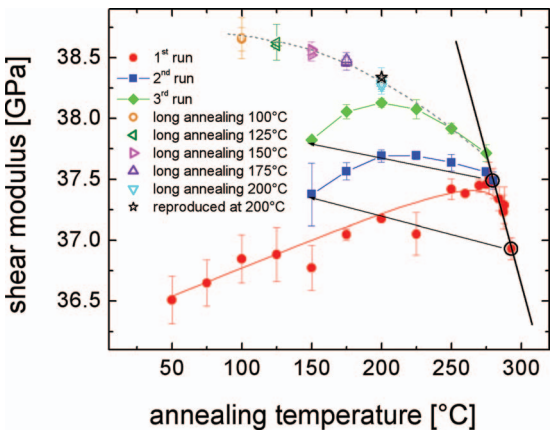

FIG. 2. (Color) Shear modulus vs annealing temperature for a freshly prepared $Pd_{40}Ni_{40}P_{20}$ bulk metallic glass with subsequent annealing procedure.

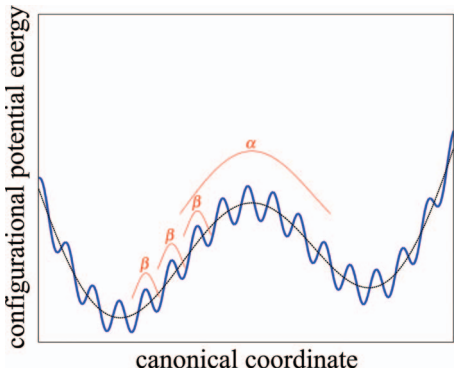

FIG. 3. (Color) Schematic diagram of the potential energy landscape showing a typical α barrier and β steps within a metabasin.

The G value of 38.3 GPa at 200 °C can be reproduced, within the error of the measurement, independently from the thermodynamic path. We demonstrate that by annealing the sample at lower temperatures for times between 8 h (175 °C) and 15 h (125 °C)—(open symbols in Fig. 2) and then going back to 200 °C for 17 h. The reproduction and path-independence of the G values can be obtained as long as the α-relaxation process is not initiated. We can also identify the trend revealed by this set of data that shows G to decrease from 38.65 to 38.3 GPa between 100 and 200 °C, with a "quasiequilibrium" relaxation path that leads to the α-relaxation process. We denote this quasiequilibrium relaxation path by a dotted line in Fig. 2. Conversely, the other G-data gathered between 100 and 200 °C (or even up to 250 °C) obtained by cycling though 1 h annealing durations appear to be path dependent, as the data cannot be reproduced by sequential passes through a specific temperature. Interestingly, the G values gathered by multiple passes through a specific temperature, whether by heating or cooling, are shown to systematically increase. We identify those data points, which are associated with 1 h annealing in 25 °C intervals, or equivalently, with a cooling or heating rate of 25 °C/1 h, with dynamic or "intermediate" nonequilibrium G states. Furthermore, the systematic increase in G observed by sequential heat treatments through specific temperatures can be attributed to transient cumulative relaxation toward quasistatic relaxation. It is noted here that the sample remains fully amorphous as checked by x-ray after all heat treatments.

The observed behavior can be interpreted using the concept of sub-basin/metabasin organization of the potential energy landscape (see Fig. 3 for a schematic drawing), proposed first by Goldstein and later refined by Debenedetti and Stillinger.[15] When quenched rapidly from the melt the system falls out of equilibrium and freezes in a configuration that corresponds to a position high up within a metabasin. Annealing the sample thermally activates barrier crossings up to a certain level of barrier heights, and depending on that energy level, the sample may or may not be allowed to relax into a different state. Such different state may be a different stable configurational state, which represents the case in which the system irreversibly escapes the original (inherent) metabasin and lands in a different metabasin (α-relaxation), or a different "quasistable" liquid state. Since heat treatments at temperatures far below the glass transition provide only

small amounts of thermal energy, the excitation will usually be too small to carry the system into a different metabasin with a different configuration (α-relaxation). Instead, depending on the duration of the heat treatment, either reversible quasiequilibrium or dynamic nonequilibrium states may be attained by thermal activation at these temperatures. Thus depending on the duration of the annealing treatments at low temperatures (or the cooling/heating rate), the system will either relax into discrete quasiequilibrium sub-basins by so called β-relaxation events,[2,8] or attain other dynamic nonequilibrium states. Since the potential energy that corresponds to the as-cast state tends to be high up in the inherent metabasin, any subsequent annealing will tend to decrease the system's potential energy as the system sinks further down into the inherent metabasin. Lower-energy states within a metabasin, whether quasistatic or dynamic, should be associated with a larger average curvature below the inflection point (see Fig. 3) in the potential energy landscape and thus a larger shear modulus. It is therefore conceivable that successive annealing processes that lead to a different dynamic or quasiequilibrium state at low temperatures will result in incrementally higher shear modulus.

In summary, we present shear modulus measurements acquired for a bulk $Pd_{40}Ni_{40}P_{20}$ glass subjected to sequential thermal annealing treatments, which were performed over temperatures that range from well below the glass transition to slightly above, and for durations that range from shorter than the β-relaxation time to slightly longer than an α-relaxation time. After short-duration annealing treatments, the system was found frozen in instantaneous shear-modulus states, which were found to be irreversible and associated with incrementally higher values. These instantaneous states have been identified with dynamic nonequilibrium states within the inherent glass metabasin. After long-duration treatments, the system was found relaxed at quasistationary shear modulus states. These quasiequilibrium states have been identified with distinct potential energy minima (sub-basins) within the inherent glass metabasin, and the processes that lead to these states have been identified with β-relaxation events.

Financial support is acknowledged by the DFG-SFB 602 and Sa 337/10-1 Leibniz-Program as well as the MRSEC Program of the National Science Foundation under Award No. DMR-0520565.

[1]W. L. Johnson and K. Samwer, Phys. Rev. Lett. **95**, 195501 (2005); M. D. Demetriou, J. S. Harmon, M. Tao, G. Duan, K. Samwer, and W. L. Johnson, *ibid.* **97**, 065502 (2006); M. L. Lind, G. Duan, and W. L. Johnson, *ibid.* **97**, 015501 (2006); M. Zink, K. Samwer, W. L. Johnson, and S. G. Mayr, Phys. Rev. B **73**, 172203 (2006); M. Zink, K. Samwer, W. L. Johnson, and S. G. Mayr, *ibid.* **74**, 012201 (2006); G. Duan, M. L. Lind, M. D. Demetriou, W. L. Johnson, W. A. Goddard III, T. Cagin, and K. Samwer, Appl. Phys. Lett. **89**, 151901 (2006); W. L. Johnson, M. D. Demetriou, J. S. Harmon, M. L. Lind, and K. Samwer, MRS Bull. **32**, 644 (2007).
[2]P. Lunkenheimer, U. Schneider, R. Brand, and A. Loidl, Contemp. Phys. **41**, 15 (2000); P. Rösner, K. Samwer, and P. Lunkenheimer, Europhys. Lett. **68**, 226 (2004); J. Hachenberg and K. Samwer, J. Non-Cryst. Solids **352**, 5110 (2006).
[3]J. Hachenberg, D. Bedorf, K. Samwer, R. Richert, A. Kahl, M. D. Demetriou, and W. L. Johnson, Appl. Phys. Lett. **92**, 131911 (2008).
[4]R. Brüning and K. Samwer, Phys. Rev. B **46**, 11318 (1992).
[5]R. Rambousky, M. Moske, and K. Samwer, Z. Phys. B: Condens. Matter **99**, 387 (1996); M. Weiss, M. Moske, and K. Samwer, Phys. Rev. B **58**, 9062 (1998).
[6]H. Vogel, Phys. Z. **22**, 645 (1921); G. S. Fulcher, J. Am. Ceram. Soc. **8**, 339 (1925); G. Tammann and W. Hesse, Z. Anorg. Allg. Chem. **156**, 245 (1926); M. D. Ediger, C. A. Angell, and S. R. Nagel, J. Phys. Chem. **100**, 13200 (1996).
[7]T. Hecksher, A. I. Nielsen, N. Olsen, and J. C. Dyre, Nat. Phys. **4**, 737 (2008).
[8]R. Richert and K. Samwer, New J. Phys. **9**, 36 (2007).
[9]K. Bothe and H. Neuhäuser, Scr. Metall. **16**, 1053 (1982); B. Porscha and H. Neuhäuser, Scr. Metall. Mater. **32**, 931 (1995).
[10]C. Nagel, K. Rätzke, E. Schmidtke, F. Faupel, and W. Ulfert, Phys. Rev. B **60**, 9212 (1999).
[11]H. Teichler, Phys. Rev. E **71**, 031505 (2005); H. R. Schober, Physica A **201**, 14 (1993).
[12]J. S. Harmon, M. D. Demetriou, W. L. Johnson, and K. Samwer, Phys. Rev. Lett. **99**, 135502 (2007).
[13]J. D. Eshelby, Proc. R. Soc. London, Ser. A **241**, 376 (1957); **252**, 1271 (1959).
[14]V. A. Khonik, Yu. P. Mitrofanov, S. A. Lyakov, D. A. Khoviv, and R. A. Konchakov, J. Appl. Phys. **105**, 123521 (2009).
[15]M. Goldstein, J. Chem. Phys. **51**, 3728 (1969); P. G. Debenedetti and F. H. Stillinger, Nature (London) **410**, 259 (2001).